Published OnlineFirst September 9, 2011; DOI:10.1158/1078-0432.CCR-11-0313

The expression of *GAPDH* was measured as an internal control.

Quantitative real-time PCR

cDNA from primary NBLs and cell lines were subjected to the real-time PCR to quantitate the expression levels of *MYCN*, *Miz-1*, and *NLRR3* mRNA. TaqMan GAPDH control reagent kit (Perkin-Elmer Applied Biosystems) was used for *GAPDH* expression and analyzed by an ABI prism 7500 Sequence Detection System (Applied Biosystems). *NLRR3* and *Miz-1* TaqMan probes were purchased from Applied Biosystems. *MYCN* mRNA expression was measured by the SYBR green real-time PCR system. The primers and probes used for real-time PCR were listed in Supplementary Table S4.

Generation of a specific antibody against NLRR3

The rabbit polyclonal anti-NLRR3 antibody was raised against a mixed synthetic peptide corresponding to amino acid sequences between positions 655 to 670 and 692 to 707 of human NLRR3. The peptide and polyclonal antibody (TB0266) were generated by Medical and Biological Laboratories (Nagoya, Japan). The specificity of the affinity-purified antibody was assayed by immunoblotting.

Plasmid constructs

The protein-coding region of *Miz-1* was amplified by PCR and inserted into the *Eco*RI site of pcDNA3.1 (Invitrogen) flanked with a Flag tag. The human *NLRR3* promoter region and its 5′ progressive deletion mutant were amplified by PCR and then inserted into the *Sacy* site in the upstream of the luciferase gene of the pGL3-basic plasmid (Promega). All constructs were verified by DNA sequencing. The pUHD-MYCN vector was kindly provided by Dr. M. Schwab (German Cancer Research Center, Heidelberg, Germany).

Luciferase reporter assay

SH-SY5Y cells were seeded at a density of 5×10^4 cells/12-well cell culture plate and allowed to attach overnight. The cells were transiently cotransfected with each mutant of the human *NLRR3* promoter-driven luciferase reporter and an internal control vector for *Renilla* luciferase, or a combination of the indicated expression vectors. The total amount of plasmid DNA per transfection was kept consistent with the pcDNA3.1 vector. Both firefly and *Renilla* luciferase activities were assayed with the Dual-Luciferase reporter assay system (Promega) according to the manufacturer's instructions. The firefly luminescence signal was normalized on the basis of the *Renilla* luminescence signal.

siRNA transfection

To knockdown endogenous MYCN expression, SK-N-AS, SK-N-BE, and SH-SY5Y cells were transfected with 10 nmol/L of the indicated siRNA purchased from Dharmacon by using LipofectAMINE RNAiMAX (Invitrogen), according to the manufacturer's recommendations. The list of siRNA sequences used will be provided upon request. Forty-eight hours after transfection, cell lysates were prepared and analyzed for the expression levels of NLRR3 and MYCN by immunoblotting.

Immunoblot analysis

The cells were washed twice with ice-cold PBS and then lysed immediately with SDS sample buffer containing 10% glycerol, 5% β-mercaptoethanol, 2.3% SDS, and 62.5 mmol/L Tris-HCl (pH 6.8). The protein concentrations were determined by using Bio-Rad protein assay dye reagent (Bio-Rad Laboratories). Equal amounts of cell lysates were separated by SDS-PAGE and electrophoretically transferred onto Immobilon-P membranes (Millipore). The transferred membranes were blocked with 5% nonfat dry milk in TBS containing 0.1% Tween-20 and incubated with appropriate primary antibodies at room temperature for 1 hour followed by incubation with horseradish peroxidase–conjugated goat anti-mouse or anti-rabbit secondary antibodies (Cell Signaling Technology Inc.) at room temperature for 1 hour. Immunoreactive bands were visualized by an ECL system (GE Healthcare). The primary antibodies used in this study were as follows: monoclonal anti-MYCN (Ab-1; Oncogene Research Products), polyclonal anti-NLRR3, polyclonal anti–Miz-1 (Santa Cruz Biotechnology), monoclonal anti-GAP43 (9-1E21; Chemicon), and polyclonal anti-actin (20-33; Sigma) antibodies.

Chromatin immunoprecipitation assays

A chromatin immunoprecipitation (ChIP) assay was carried out according to the protocol provided by Upstate Biotechnology (Charlottesville). In brief, cells were cross-linked with 1% formaldehyde in medium for 10 minutes at 37°C. Chromatin solutions were prepared and immunoprecipitated with the following antibodies: anti-MYCN, anti–Miz-1, anti-Max rabbit polyclonal antibodies (Santa Cruz Biotechnology), and normal mouse or rabbit serum as a control. The immunoprecipitates were eluted with 100 μL of elution buffer (1% SDS and 1 mmol/L $NaHCO_3$). Formaldehyde-mediated cross-links were reversed by heating at 65°C for 4 hours, and the reaction mixtures were treated with proteinase K at 45°C for 1 hour. DNAs of the immunoprecipitates and control input DNAs were purified by using a QIAquick PCR purification kit (Qiagen). Purified DNA was subjected to optimized semiquantitative PCR amplification protocol for NLRR3 gene promoter and control regions, using appropriate primer sets (Supplementary Table S4).

Statistical analysis

Student *t* tests were employed to examine the possible association between *NLRR3* expression and other prognostic factors. The classification of high and low levels of *NLRR3*, *Miz-1*, and *MYCN* expression was determined on the basis of the mean value obtained from quantitative real-time PCR analysis. Kaplan–Meier survival curves were calculated, and survival distributions were compared by using the log-rank test. Cox regression models were used to search associations along with *NLRR3* expression, *MYCN*

Published OnlineFirst September 9, 2011; DOI:10.1158/1078-0432.CCR-11-0313

expression, *Miz-1* expression, age, *MYCN* amplification status, INSS, *TrkA* expression, DNA index, origin, and survival. Statistical significance was considered if P value was less than 0.05. The statistical analysis was carried out by SPSS Statistical Software release 12.0.

Results

NLRR3 is upregulated during neuronal differentiation

It has been previously reported that the NBL cell lines exposed to ATRA undergo neuronal differentiation (32), accompanied by a marked decrease in the expression levels of *MYCN* (33). To examine the possible involvement of MYCN in the regulation of NLRR3 expression, the NBL-derived RTBM1 cells were treated with or without 5 μmol/L ATRA. As previously described (34), RTBM1 cells underwent neuronal differentiation with extensive neurite outgrowth in response to ATRA treatment (Fig. 1A). The induced differentiation was confirmed by the expression levels of *GAP43*, a marker of neuronal differentiation (35), which increased after ATRA treatment at both mRNA and protein levels (Fig. 1B and C). As expected, MYCN expression was significantly decreased after ATRA treatment and almost diminished at 6 days after treatment. Consistent with our previous observations (23), *NLRR3* was markedly upregulated at the mRNA and protein levels during the differentiation process. Similar results were also obtained from ATRA-treated SH-SY5Y cells (Supplementary Fig. S1A and B).

Inverse correlation between *MYCN* and *NLRR3* expressions

To further confirm a possible relationship between MYCN and NLRR3, we used MYCN-inducible SHEP21N cells originally derived from NBL (36) and treated with tetracycline to switch off the expression of MYCN. As shown in Fig. 2A, the reduced expression level of *MYCN* upon tetracycline treatment was confirmed by reverse transcriptase PCR (RT-PCR) and immunoblotting, whereas NLRR3 expression was increased after tetracycline treatment.

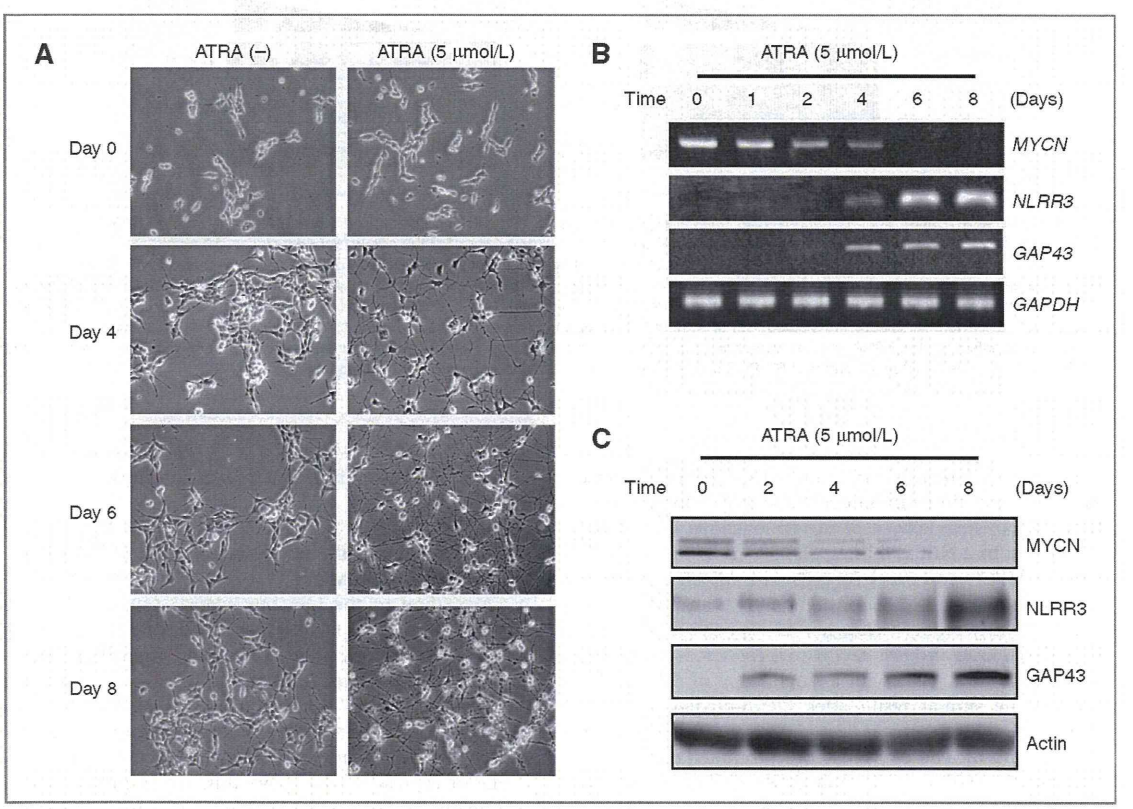

Figure 1. Opposite expression pattern of *NLRR3* and *MYCN* in differentiated RTBM1 cells in response to ATRA. A, ATRA-induced differentiation program in RTBM1 cells. Cells were treated with 5 μmol/L ATRA or left untreated. At the indicated time-periods after treatment with ATRA, neurite outgrowth was examined with a phase-contrast microscope. B and C, RT-PCR and immunoblot analysis for MYCN, NLRR3, and GAP43 in response to ATRA. RTBM1 cells were treated as in A. Total RNA and cell lysates were prepared and processed for RT-PCR (B) and immunoblotting with indicated antibodies (C). For RT-PCR, *GAPDH* was used as an internal control. For immunoblotting, actin was used as a loading control.

Published OnlineFirst September 9, 2011; DOI:10.1158/1078-0432.CCR-11-0313

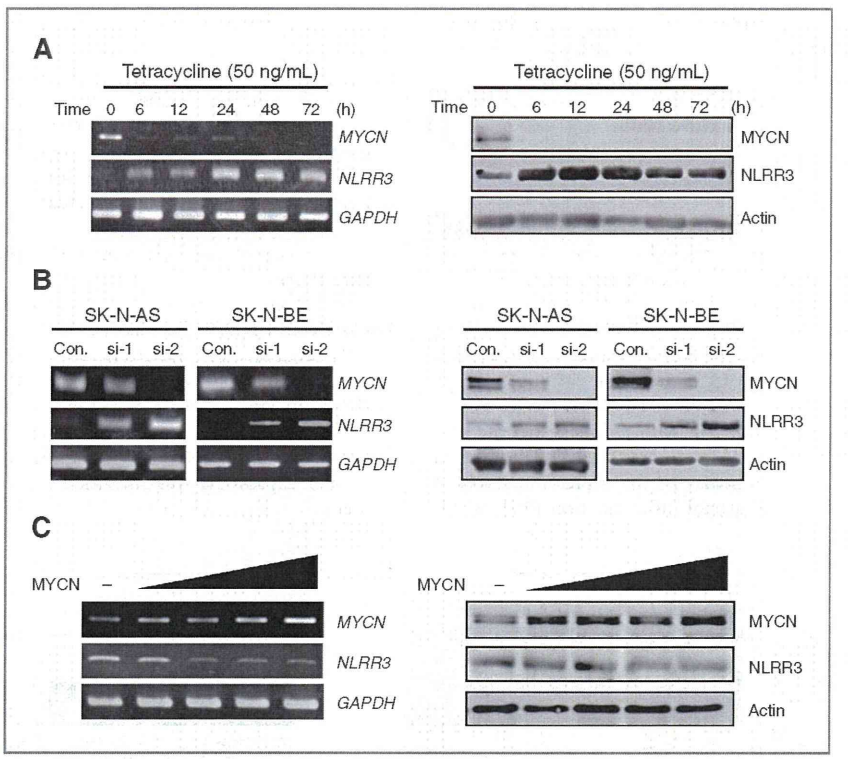

Figure 2. Inverse regulation of MYCN and NLRR3 in various NBL cell lines. A, RT-PCR and immunoblot analysis for MYCN and NLRR3 in SHEP21N cells maintained in the presence of tetracycline. At the indicated time points after the addition of tetracycline (50 ng/mL), total RNA and cell lysates were prepared and processed for RT-PCR (left) and immunoblotting with indicated antibodies (right). B, siRNA-mediated knockdown of the endogenous MYCN. SK-N-AS and SK-N-BE cells were transfected with control siRNA (Con.) or with 2 siRNA (si-1 and si-2) against MYCN. At 48 hours after transfection, total RNA and cell lysates were prepared and processed for RT-PCR (left) and immunoblotting with indicated antibodies (right). C, SH-SY5Y cells were transiently transfected with or without the increasing amounts of the expression plasmid encoding MYCN. Forty-eight hours after transfection, total RNA and cell lysates were prepared and processed for RT-PCR (left) and immunoblotting (right) with indicated antibodies. *GAPDH* was used as an internal control of RT-PCR and actin was used as a loading control for immunoblotting.

To examine whether MYCN and NLRR3 have an inverse functional relationship under these physiologic conditions, siRNA knockdown of the endogenous MYCN was carried out in 2 NBL cell lines, SK-N-AS cells with a single copy of *MYCN* and SK-N-BE cells with *MYCN* amplification. As shown in Fig. 2B, one of the siRNAs against *MYCN*, si-2, efficiently reduced endogenous expression of *MYCN* in both cell lines and resulted in an increased expression of NLRR3. SH-SY5Y cells with a single copy of *MYCN* also showed the similar result after siRNA-mediated knockdown of the endogenous MYCN (Supplementary Fig. S2A and B). These observations prompted us to examine whether MYCN can directly downregulate *NLRR3* expression. To address this issue, SH-SY5Y NBL cells were transfected with the expression plasmid encoding the *MYCN* gene. Forced expression of MYCN resulted in a dose-dependent decrease of NLRR3 expression both at the mRNA and protein levels (Fig. 2C), suggesting that *NLRR3* expression is negatively regulated by MYCN in NBL cells.

MYCN represses the promoter activity of *NLRR3* in association with Miz-1

According to the previous reports (19, 20, 37), Myc proteins repress its target genes by forming a complex with Miz-1. Under these conditions at low expression levels of Myc, Miz-1 activates transcription of the target genes by cooperating with other transcriptional cofactors and enhances cell differentiation (20). Therefore, we hypothesized that Miz-1 might be involved in the regulation of *NLRR3* expression. To prove this, we examined whether exogenously expressed Miz-1 upregulates *NLRR3* expression in SH-SY5Y cells. Figure 3A, left shows that *NLRR3* expression was upregulated by overexpression of Miz-1 in the same manner as a positive control, $p15^{Ink4b}$ expression, whereas expression of other NLRR family members, *NLRR1*

Published OnlineFirst September 9, 2011; DOI:10.1158/1078-0432.CCR-11-0313

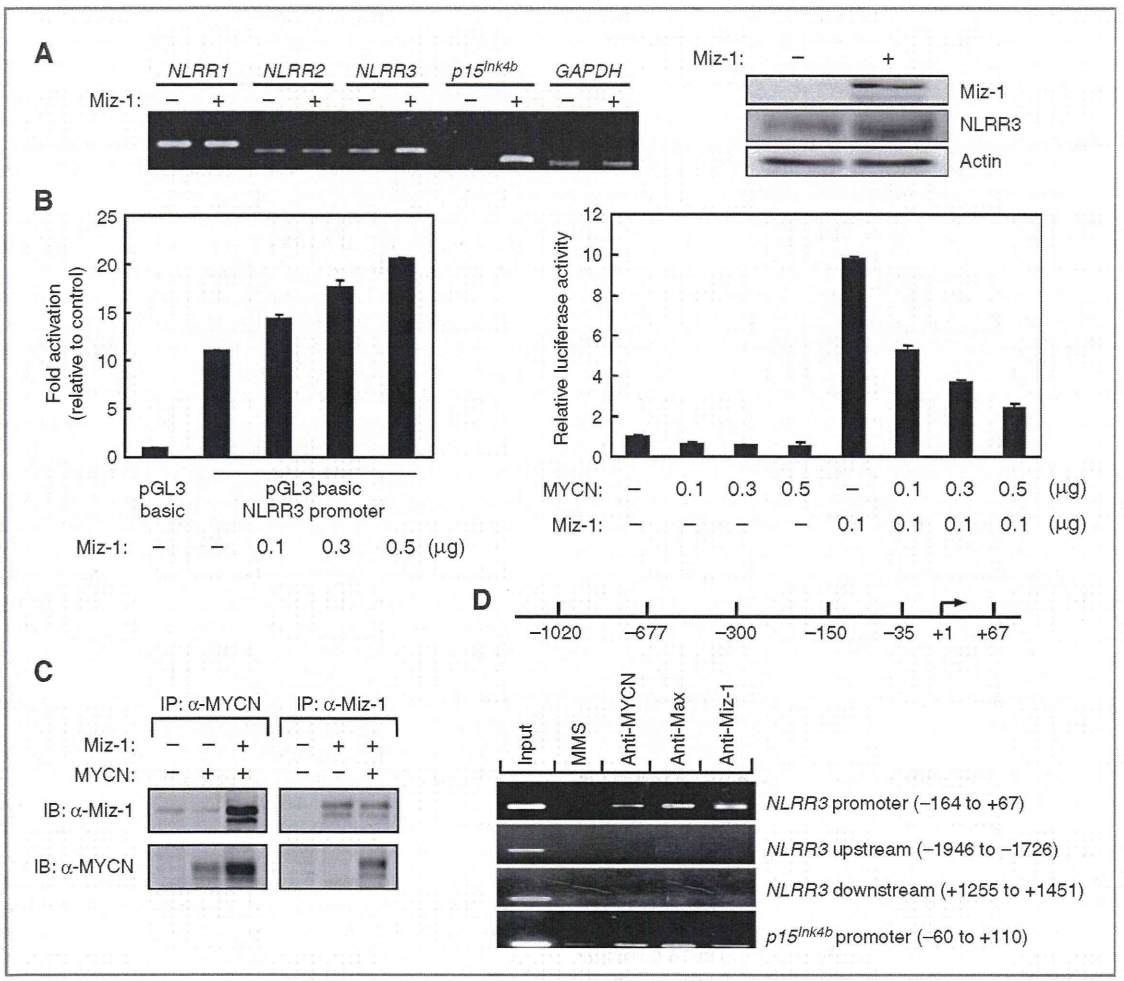

Figure 3. Regulation of the *NLRR3* promoter by MYCN and Miz-1. A, left, RT-PCR analysis showing expression of *NLRR1*, *NLRR2*, *NLRR3*, and $p15^{INK4b}$ in SH-SY5Y cells transiently transfected either with control or Miz-1–expressed plasmid. *GAPDH* was used as an internal control. Right, Western blot showing expression of *NLRR3* and *Miz-1* in SH-SY5Y cells transiently transfected either with control vector or with Miz-1 expressing vector. Actin was used as a loading control. B, left, Miz-1 enhances promoter activity of *NLRR3* in transient transfection assay. Data represent fold activation of the *NLRR3* promoter (−677 to +67) construct upon coexpression of increasing amounts of the expression plasmid for Miz-1 in SY5Y cells. Forty-eight hours after transfection, the cells were lysed and their relative luciferase activities were measured. Firefly luminescence signal was normalized on the basis of *Renilla* luminescence signal. Right, expression of MYCN reduces the basal activity of the *NLRR3* promoter and abrogates transactivation by Miz-1. SH-SY5Y cells were transiently cotransfected with or without constant amount of the expression plasmid for the Miz-1 and 0.1 μg of *NLRR3* promoter (−677 to +67) together with or without the increasing amounts of the expression plasmid for MYCN. The luciferase activity was determined as in B, left. Results are the mean of 3 independent experiments ± SD. C, interaction between MYCN and Miz-1 in NBL cells. Whole cell lysates prepared from SK-N-AS cells transfected with indicated vectors and immunoprecipitated (IP) with the monoclonal anti-MYCN antibody or with polyclonal anti–Miz-1 antibody. The immunoprecipates were analyzed by immunoblotting (IB) with the polyclonal anti–Miz-1 antibody or with monoclonal anti-MYCN antibody, respectively. D, ChIP analysis of SH-SY5Y cells was carried out by using the indicated antibody and PCR primers specific for the different part of *NLRR3* promoter (top 3 panels), upstream, downstream (middle 2 panels) regions of the *NLRR3* gene, and for $p15^{INK4b}$ promoter (bottom).

and *NLRR2*, showed no change. The increased expression of NLRR3 protein was also confirmed by Western blot analysis (Fig. 3A, right). This induction of NLRR3 by Miz-1 was also observed in SK-N-AS cells (Supplementary Fig. S3). To determine whether Miz-1 activates the *NLRR3* promoter, the region spanning exon 2 and 5′-upstream sequences of the *NLRR3* gene (nucleotide −1,020 to +67) was cloned and analyzed for promoter activity by using a luciferase reporter assay. The promoter deletion analysis showed that a nucleotide position between −677 and +67 gives maximum promoter activity (Supplementary Fig. S4A). The core promoter region (−35 to +67) also

Published OnlineFirst September 9, 2011; DOI:10.1158/1078-0432.CCR-11-0313

showed higher promoter activity than other deletion mutants. In transient-cotransfection assays, simultaneous expression of Miz-1 increased the luciferase activities driven by the *NLRR3* promoter (−677 to +67; Fig. 3B, left).

On the contrary, overexpression of MYCN resulted in reduced activity of the *NLRR3* promoter (Supplementary Fig. S4B). These results suggest that Miz-1 and MYCN together contribute to the transcriptional regulation of the *NLRR3* gene. Indeed, the activation of the *NLRR3* promoter by exogenous Miz-1 expression in SH-SY5Y cells was suppressed by coexpression of MYCN in a dose-dependent manner (Fig. 3B, right). The luciferase activities driven by the core promoter region (−35 to +67) also showed a similar result (data not shown). It was reported that a transcriptional suppression of the MYCN-targeted genes occurs when MYCN forms a complex with Miz-1 and Max (19). To make certain of the physical interaction between MYCN and Miz-1, the whole cell lysates prepared from the SK-N-AS cells cotransfected with *MYCN* and *Miz-1* were subjected to an immunoprecipitation assay. As shown in Fig. 3C, coimmunoprecipitation using either MYCN or Miz-1 antibody confirmed that MYCN and Miz-1 formed a complex in SK-N-AS cells as previously reported in non-NBL cell lines (38). Moreover, ChIP analysis revealed that MYCN, Max, and Miz-1 were recruited onto the same promoter region of *NLRR3* (−164 to +67) in SH-SY5Y cells (Fig. 3D). Hence, MYCN negatively regulates *NLRR3* expression by forming a transcriptional complex with Miz-1 in NBL cells.

Increased expression of *NLRR3* and *Miz-1* in favorable neuroblastoma

In our previous report, *NLRR3* is highly expressed in favorable NBLs with a single copy of *MYCN* as compared with NBLs with *MYCN* amplification. To evaluate whether the expression pattern of *Miz-1*, *NLRR3*, and *MYCN* observed in NBL cell lines is consistent in primary NBLs, we analyzed expression levels of those 3 genes in 16 favorable (stages 1 or 2, high expression of *TrkA* and a single copy of *MYCN*) and 16 unfavorable (stages 3 or 4, low expression of TrkA and amplification of *MYCN*) NBL samples by semiquantitative RT-PCR. As shown in Supplementary Fig. S5A, *NLRR3* and *Miz-1* were expressed at higher levels in favorable NBLs than those in unfavorable tumors, whereas the levels of *MYCN* expression were predominantly high in the unfavorable tumors. The expression levels of *NLRR3* and *Miz-1* were also higher in the cell lines with a single copy of *MYCN* than those with *MYCN* amplification, indicating evidence of a positive correlation between *NLRR3* and *Miz-1* expressions and of an inverse correlation between *NLRR3* and *MYCN* expressions (Supplementary Fig. S5B). Those expression patterns were further assessed by immunohistochemistry for NLRR3, MYCN, and Miz-1 in primary NBL tissues (Supplementary Fig. S5C). We carried out immunohistochemical staining on all 11 available paraffin-embedded primary NBL tissues, including 5 NBLs with a single copy of *MYCN* and favorable histology according to INPC (39), 3 NBLs carrying a single copy of *MYCN* with unfavorable histology, and 3 NBLs with *MYCN* amplification and unfavorable histology. As shown in Supplementary Fig. S5C and Supplementary Table S1, the absence of MYCN amplification was associated with strong positive staining of NLRR3 and Miz-1 in all examined samples except one (case 8). All 3 NBLs with *MYCN* amplification showed weak staining for both NLRR3 and Miz-1.

Low expression of *NLRR3* and *Miz-1* is associated with an unfavorable outcome of neuroblastoma

To evaluate whether a statistically significant relationship exists between the patients' survival periods and the expression of *NLRR3*, *Miz-1*, or *MYCN* in primary NBLs, we quantitatively measured the expression levels of *NLRR3*, *Miz-1*, and *MYCN* mRNAs in 87 primary NBLs by using the quantitative real-time PCR method. The clinical features of each NBL samples are listed in Supplementary Table S2. As shown in Table 1, high levels of *NLRR3* expression were significantly associated with younger age ($P = 0.047$), single copy of *MYCN* ($P = 0.047$), favorable disease stages ($P = 0.041$), high levels of *TrkA* expression ($P = 0.042$), and diploid DNA index ($P = 0.003$), but not with tumor origin ($P = 0.933$). A high level of *Miz-1* expression was also significantly associated with younger age ($P = 0.004$), single copy of *MYCN* ($P = 0.004$), favorable disease stages ($P = 0.001$), and high levels of *TrkA* expression ($P = 0.001$), but not with DNA index ($P = 0.060$) and tumor origin ($P = 0.959$). In contrast, a high level of *MYCN* expression was significantly associated with *MYCN* amplification ($P = 0.0001$), advanced disease stages ($P = 0.0031$), low levels of *TrkA* expression ($P = 0.026$), and tumor origin ($P = 0.028$), but not with DNA index ($P = 0.079$), which is consistent with the previous reports (23, 40, 41). There was also a marginal association with patient age ($P = 0.063$). These results suggest that high expression of *NLRR3* and *Miz-1* is well associated with conventional prognostic markers predicting a favorable NBL outcome.

To examine whether the expression levels of *NLRR3*, *Miz-1* and/or *MYCN* have a prognostic significance in primary NBLs, we employed log-rank tests for gene-expression data (Supplementary Table S3). There were significant differences in survival rates in the groups of patients with high and low expression of *NLRR3*, *Miz-1*, and *MYCN*. Patients with high expression of *NLRR3* or *Miz-1* had a higher survival rate than patients with low expression of *NLRR3* or *Miz-1*, and such a difference in survival rate was statistically significant ($P = 0.0023$ and $P = 0.00060$, respectively). However, a patient with high *MYCN* expression was associated with a lower survival rate than that of the *MYCN* low subset ($P < 0.00001$; Supplementary Table S3). Figure 4 shows Kaplan–Meier cumulative survival curves for 87 patients with NBL in terms of expression of *NLRR3*, *Miz-1* and *MYCN*. High expression of *NLRR3* and that of *Miz-1* were significantly associated with good survival ($P = 0.0023$ and $P = 0.00060$, respectively; Fig. 4A, left and right). As already known, high expression of *MYCN*

Published OnlineFirst September 9, 2011; DOI:10.1158/1078-0432.CCR-11-0313

Table 1. Correlation between expression of *NLRR3* or *MYCN* or *Miz-1* and other prognostic factors (Student *t* test)

		NLRR3		*MYCN*		*Miz-1*	
Variable	**No.**	**Mean ± SEM**	***P***	**Mean ± SEM**	***P***	**Mean ± SEM**	***P***
Age, y							
<1	32	0.043 ± 0.011	0.047[a]	0.034 ± 0.013	0.063	0.091 ± 0.019	0.004[a]
≥1	55	0.024 ± 0.003		0.141 ± 0.043		0.042 ± 0.007	
MYCN copy number							
Single copy	58	0.041 ± 0.006	0.047[a]	0.022 ± 0.016	0.0001[a]	0.077 ± 0.012	0.004[a]
Amplified	29	0.019 ± 0.004		0.222 ± 0.053		0.026 ± 0.004	
Tumor stage							
1, 2, 4s	34	0.043 ± 0.009	0.041[a]	0.007 ± 0.002	0.0031[a]	0.093 ± 0.017	0.001[a]
3, 4	53	0.024 ± 0.003		0.144 ± 0.036		0.039 ± 0.007	
TrkA expression							
High	24	0.047 ± 0.013	0.042[a]	0.009 ± 0.003	0.026[a]	0.104 ± 0.024	0.001[a]
Low	61	0.025 ± 0.004		0.125 ± 0.032		0.044 ± 0.006	
DNA index							
Diploidy	42	0.019 ± 0.003	0.003[a]	0.121 ± 0.037	0.079	0.049 ± 0.008	0.06
Aneuploidy	31	0.050 ± 0.010		0.034 ± 0.023		0.085 ± 0.019	
Tumor origin							
Adrenal gland	48	0.032 ± 0.007	0.933	0.135 ± 0.035	0.028[a]	0.059 ± 0.012	0.959
Others	39	0.032 ± 0.004		0.034 ± 0.025		0.060 ± 0.011	

[a]$P < 0.05$.

was strongly associated with a poor prognosis of NBL ($P < 0.00001$; Fig. 4A, middle). Remarkably, the combination of low levels of both *NLRR3* and *Miz-1* expressions showed a significantly worse prognosis as compared with the other combination, high *NLRR3* and *Miz-1* expressions ($P = 0.0012$; Fig. 4C). Furthermore, the combination of low expression of *NLRR3* and high expression of *MYCN* showed a significantly worse prognosis than the combination of high expression of *NLRR3* and low expression of *MYCN* ($P < 0.00001$; Fig. 4B). In NBLs with low expression of *MYCN*, the expression levels of *NLRR3* could segregate the prognosis into good and intermediate groups.

The univariate Cox regression analysis shown in Table 2 was employed to examine the individual relationship of each variable to survival. The results in Table 2 showed that *NLRR3* expression, *MYCN* expression, *Miz-1* expression, age, *MYCN* amplification, stage *TrkA* expression, and origin were of prognostic importance, supporting the results of the log-rank test. Moreover, the multivariate Cox models were fitted to assess the predictive importance of NLRR3 expression for survival after controlling other prognostic factors. The results in Table 2 showed that *NLRR3* expression was significantly associated with survival after controlling *TrkA* expression ($P = 0.0212$), suggesting that *NLRR3* expression was an independent prognostic factor from *TrkA* expression (Table 2). This suggests that *NLRR3* expression is associated with survival after controlling *MYCN* expression ($P = 0.0610$), *Miz-1* expression ($P = 0.1510$), *MYCN* amplification ($P = 0.1210$), and stage ($P = 0.1040$), and also supports that *NLRR3* expression could serve as a prognostic biomarker for NBL tumors dependent on both MYCN and Miz-1 expression as well as *MYCN* amplification.

Discussion

In primary human NBLs, *MYCN* is frequently amplified and thereby one of the most important prognostic factors. In this study, we found that *NLRR3* is a direct target of MYCN but its expression is negatively regulated by MYCN in association with Miz-1. In primary NBLs, both *NLRR3* and *Miz-1* are expressed at significantly high levels in favorable NBLs and downregulated in *MYCN*-amplified aggressive tumors.

In general, favorable NBL cells show more differentiated features than unfavorable cells (30). The treatment of NBL cells with ATRA induces neuronal differentiation accompanied with growth inhibition and reduction of *MYCN* expression (33). Under such conditions, *NLRR3* is induced while *MYCN* is decreased (Figs. 1 and 2). These results suggest a functional inverse relationship between MYCN and NLRR3 in cellular differentiation and tumor development. In some NBL cell lines, siRNA-mediated knockdown of endogenous MYCN caused NLRR3 induction; conversely, ectopic expression of MYCN resulted in a decreased expression of *NLRR3*. Hence, the inverse regulatory relationship between NLRR3 and MYCN may be present as a

Published OnlineFirst September 9, 2011; DOI:10.1158/1078-0432.CCR-11-0313

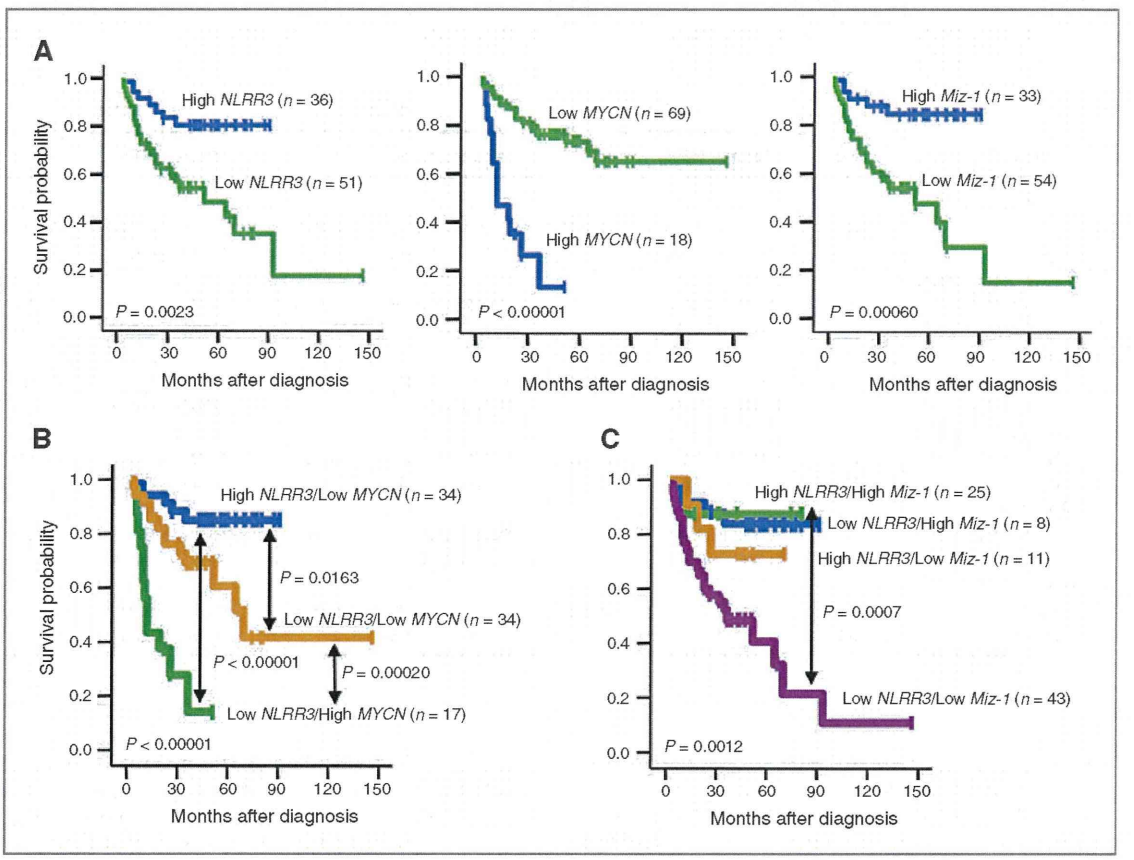

Figure 4. Real-time PCR analysis for the expression of *NLRR3*, *MYCN*, and *Miz-1* in 87 primary NBLs. Kaplan–Meier survival curves of patients with NBLs on the basis of higher or lower expression levels of *NLRR3* (A, left); *MYCN* (A, middle); *Miz-1* (A, right); *NLRR3* and *MYCN* (B); or *NLRR3* and *Miz-1* (C). In case of *NLRR3* and *MYCN* survival curve, high NLRR3/high MYCN group was excluded because this group consists of only 2 samples. Relative expression levels of *NLRR3* or *MYCN* or *Miz-1* mRNA were determined by calculating the ratio between *GAPDH* and *NLRR3* or *MYCN* or *Miz-1*.

consequence of MYCN-induced transcriptional downregulation of *NLRR3*.

MYCN protein is an important regulator of many cellular processes, including growth, proliferation, differentiation, and apoptosis (42). A part of these diverse cellular functions of MYCN may be due to the combined abilities of both activating and repressing transcription of the target genes (42). Transcriptional activation by MYCN occurs *via* dimerization with its partner protein, Max, and direct binding to specific DNA sequences named E-boxes. MYCN directly binds and stimulates the expression of approximately 4,000 of the E-box containing genes (43). Although heterodimerization of Max with MYCN is necessary to regulate gene expression, the other proteins including *Miz-1* may bind to C-terminal MYCN in addition to Max (19, 20, 44). Concurrent binding of these factors redirects the MYCN/Max dimer to noncanonical sites such as the initiator element, where this complex might prevent the efficient binding of basal transcriptional machinery or coactivators necessary for transactivation, resulting in repression of gene expression (38, 44). The dimerization with MYCN switches Miz-1 from a transcriptional activator to a repressor of the target genes, likely by preventing the interaction of Miz-1 with its own coactivator (19, 20). Several studies have shown that Miz-1 binds and activates the promoter of several genes, including $p15^{INK4b}$ and $p21^{CIP1}$, and the transactivation can be negatively regulated by its association with MYCN (16, 17, 29). Regarding the reduction of NLRR3 expression observed in this study, Miz-1 seems to be a key molecule forming a transcription factor complex with MYCN. Because Miz-1 itself acts as an activator of *NLRR3* promoter, *NLRR3* expression may be switched on and off through Miz-1 in the absence and presence of MYCN, respectively. Although the expression levels of Miz-1 in unfavorable NBLs are relatively low, its amount still may be enough to act with MYCN to inhibit transactivation of *NLRR3* in NBLs.

Published OnlineFirst September 9, 2011; DOI:10.1158/1078-0432.CCR-11-0313

Table 2. Multiple Cox regression model using NLRR3 expression and dichotomous factors of MYCN expression, Miz-1 expression, age, MYCN amplification, stage, TrkA expression, and origin ($n = 87$)

Model	Factor	*P*	HR (95% CI)
Univariate analysis			
A	*NLRR3* mRNA expression (high vs. low)	0.0041[a]	0.291 (0.125–0.678)
B	*MYCN mRNA* expression (high vs. low)	<0.0001[a]	5.050 (2.450–10.40)
C	*Miz-1* mRNA expression (high vs. low)	0.0021[a]	0.212 (0.080–0.561)
D	Age (≥1 vs. <1 y)	0.0161[a]	0.309 (0.119–0.803)
E	*MYCN* amplification (single copy vs. amplified)	<0.0001[a]	4.628 (2.281–9.387)
F	Stage (1,2,4s vs. 3,4)	0.0010[a]	12.66 (3.023–53.09)
G	*TrkA* expression (high vs. low)	0.0070[a]	7.180 (1.714–30.07)
H	Origin (adrenal gland vs. others)	0.0480[a]	2.125 (1.005–4.491)
Multivariate analysis			
A	*NLRR3* mRNA expression (high vs. low)	0.061	0.424 (0.172–1.041)
	MYCN mRNA expression (high vs. low)	0.0011[a]	3.707 (1.735–7.921)
B	*NLRR3* mRNA expression (high vs. low)	0.151	0.503 (0.198–1.283)
	Miz-1 mRNA expression (high vs. low)	0.0301[a]	0.304 (0.104–0.893)
C	*NLRR3* mRNA expression (high vs. low)	0.0150[a]	0.347 (0.148–0.814)
	Age (≥1 vs. <1 y)	0.053	0.384 (0.146–1.013)
D	*NLRR3* mRNA expression (high vs. low)	0.121	0.545 (0.253–1.173)
	MYCN amplification (single copy vs. amplified)	0.0001[a]	3.940 (1.893–8.203)
E	*NLRR3* mRNA expression (high vs. low)	0.104	0.493 (0.210–1.156)
	Stage (1, 2, 4s vs. 3, 4)	0.0020[a]	10.108 (2.359–43.309)
F	*NLRR3* mRNA expression (high vs. low)	0.0212[a]	0.361 (0.152–0.863)
	TrkA expression (high vs. low)	0.0163[a]	5.892 (1.395–24.901)
G	*NLRR3* mRNA expression (high vs. low)	0.0070[a]	0.308 (0.132–0.720)
	Origin (adrenal gland vs. others)	0.084	1.937 (0.914–4.104)

NOTE: All variables with 2 categories. HR shows the relative risk of death of first category relative to the second.
[a]$P < 0.05$.

Inhibition of cellular differentiation is one of the well-known biological functions of MYCN. Because differentiated NBL cells have a high expression of NLRR3 instead of MYCN, the reduced expression of NLRR3 in undifferentiated, unfavorable NBL cells may propose an important component of the mechanism by which MYCN functions against cell differentiation. As ectopic expression of NLRR3 induced morphologic changes indicative of neuronal differentiation accompanying with neurite outgrowth (data not shown), the downregulation of NLRR3 by MYCN might contribute to the well-documented stimulation of cell proliferation by MYCN. Although there are MYCN target genes that are potentially involved in cell-cycle progression, including *α-prothymosin, ornithine decarboxylase, MCM7, ID2, MDM2,* and *NLRR1* (27, 36, 45–47), suppression of NLRR3 might have an additive effect on NBL cell proliferation. Our log-rank test showed that expression of NLRR3 is well associated with a favorable prognosis, suggesting its involvement in NBL differentiation. Of more interest, NLRR3 and NLRR1 seem to function oppositely in NBL. Thus, the expression of NLRR3 is a new prognostic indicator of NBL and may be involved in regulating the biology of the tumor.

Collectively, our present findings suggest that the repression of NLRR3 mediated by MYCN requires an association with Miz-1 and also contributes to the favorable outcome of NBLs. The expression pattern of NLRR3, Miz-1, and MYCN might play an important role in defining the clinical behavior of NBLs. Because NLRR3 is an orphan receptor, the future discovery of its ligand(s) may unveil the molecular mechanism of tumorigenesis, differentiation, and proliferation of NBL. Further investigation is necessary to clarify whether NLRR3 is an important primary cue for developing novel diagnostic and therapeutic strategies against high-risk NBLs.

Disclosure of Potential Conflicts of interest

No potential conflicts of interest were disclosed.

Acknowledgments

The authors thank Drs. Y. Nakamura and E. Isogai (Chiba Cancer Center Research Institute, Chiba, Japan) for their outstanding technical assistance, and Dr. Hiroki Nagase (Chiba Cancer Center Research Institute, Chiba, Japan) and Ms. Paula D. Jones (Roswell Park Cancer Institute, Buffalo, NY) for critical reading of the article.

Published OnlineFirst September 9, 2011; DOI:10.1158/1078-0432.CCR-11-0313

Grant Support

This work was supported in part by a grant-in-aid from the Ministry of Health, Labour and Welfare for Third Term Comprehensive Control Research for Cancer (A. Nakagawara), a grant-in-aid for Scientific Research on Priority Areas from the Ministry of Education, Culture, Sports, Science and Technology, Japan (A. Nakagawara), and a grant-in-aid for Scientific Research from the Japanese Society for the Promotion of Science (A. Takatori and A. Nakagawara).

The costs of publication of this article were defrayed in part by the payment of page charges. This article must therefore be hereby marked *advertisement* in accordance with 18 U.S.C. Section 1734 solely to indicate this fact.

Received February 3, 2011; revised August 3, 2011; accepted August 9, 2011; published OnlineFirst September 9, 2011.

References

1. Westemann F, Schwab M. Genetic parameters of neuroblastomas. Cancer Lett 2002;184:127–47.
2. Brodeur GM, Nakagawara A. Molecular basis of clinical heterogeneity in neuroblastoma. Am J Pediatr Hematol Oncol 1992;14: 111–6.
3. Nakagawara A, Arima M, Azar CG, Scavarda NJ, Brodeur GM. Inverse relationship between trk expression and N-myc amplification in human neuroblastomas. Cancer Res 1992;52:1364–68.
4. Nakagawara A, Arima-Nakagwara M, Scavarda NJ, Azar CG, Cantor AB, Brodeur GM. Association between high levels of expression of the TRK gene and favorable outcome in human neuroblastoma. New Engl J Med 1993;328:847–54.
5. Nakagawara A, Azar CG, Scavarda NJ, Brodeur GM. Expression and function of TRK-B and BDNF in human neuroblastomas. Mol Cell Biol 1994;14:759–67.
6. Nakagawara A, Arima-Nakagawara M, Azar CG, Scavarda NJ, Brodeur GM. Clinical significance of expression of neurotrophic factors and their receptors in neuroblastoma. Prog Clin Biol Res 1994;385: 155–61.
7. Seeger RC, Brodeur GM, Sather H, Dalton A, Siegel SE, Wong KY, et al. Associations of multiple copies of the N-myc oncogene with rapid progression of neuroblastomas. New Engl J Med 1985;313: 1111–6.
8. Kohl NE, Gee CE, Alt FW. Activated expression of the N-myc gene in human neuroblastomas and related tumors. Science 1984;226: 1335–7.
9. Nisen PD, Waber PG, Rich MA, Pierce S, Garvin JR, Gilbert F, et al. N-myc oncogene RNA expression in neuroblastoma. J Natl Cancer Inst 1988;80:1633–7.
10. Slavc I, Ellenbogen R, Jung WH, Vawter GF, Kretschmar C, Grier H, et al. Myc gene amplification and expression in primary human neuroblastoma. Cancer Res 1990;50:1459–63.
11. Seeger RC, Wada R, Brodeur GM, Moss TJ, Bjork RL, Sousa L, et al. Expression of N-myc by neuroblastomas with one or multiple copies of the oncogene. Prog Clin Biol Res 1988;271:41–9.
12. Schwab M, Ellison J, Busch M, Rosenau W, Varmus HE, Bishop JM. Enhanced expression of the human gene N-myc consequent to amplification of DNA may contribute to malignant progression of neuroblastoma. Proc Natl Acad Sci U S A 1984;81:4940–4.
13. Cohn SL, Tweddle DA. MYCN amplification remains prognostically strong 20 years after its "clinical debut". Eur J Cancer 2004;40: 2639–42.
14. Strieder V, Lutz W. Regulation of N-myc expression in development and diseases. Cancer Lett 2002;180:107–19.
15. Kouzarides T, Ziff E. The role of the leucine zipper in the fos-jun interaction. Nature 1988;336:646–51.
16. Landschulz WH, Johnson PF, Mcknight SL. The leucine zipper: a hypothetical structure common to a new class of DNA binding proteins. Science 1988;240:1759–64.
17. Alex R, Sozeri O, Meyer S, Dildrop R. Determination of the DNA sequence recognized by the bHLH-zip domain of the N-Myc protein. Nucleic Acids Res 1992;20:2257–63.
18. Blackwood EM, Kretzner L, Eisenman RN. Myc and Max function as a nucleoprotein complex. Curr Opin Genet Dev 1992;2:227–35.
19. Staller P, Peukert K, Kiermaier A, Seoane J, Lukas J, Karsunky H, et al. Repression of p15INK4b expression by Myc through association with Miz-1. Nature Cell Biol 2001;3:392–9.
20. Wu S, Cetinkaya C, Munoz-Alonso MJ, Von der Lehr N, Bahram F, Beuger V, et al. Myc represses differentiation-induced p21CIP1 expression via Miz-1-dependent interaction with the p21 core promoter. Oncogene 2003;22:351–60.
21. Zhang J, Li F, Liu X, Shen L, Liu J, Su J, et al. The repression of human differentiated-related gene NDRG2 expression by Myc via Miz-1 dependent interaction with the NDRG2 core promoter. J Biol Chem 2006;281:39159–68.
22. Koppen A, Ait-Aissa R, Hopman S, Koster J, Haneveld F, Versteeg R, et al. Dickkopf-1 is down-regulated by MYCN and inhibits neuroblastoma cell proliferation. Cancer Lett 2007;256:218–28.
23. Hamano S, Ohira M, Isogai E, Nakada K, Nakagawara A. Identification of novel human neuronal leucine-rich repeat (hNLRR) family genes and inverse association of expression of Nbla10449/hNLRR-1 and Nbla10677/hNLRR-3 with the prognosis of primary neuroblastomas. Int J Oncol 2004;24:1457–66.
24. Ohira M, Morohashi A, Inuzuka H, Shishikura T, Kawamoto T, Kageyama H, et al. Expression profiling and characterization of 4200 genes cloned from primary neuroblastomas: identification of 305 genes differentially expressed between favorable and unfavorable subsets. Oncogene 2003;22:5525–36.
25. Hayata T, Uochi T, Asashima M. Molecular cloning of XNLRR-1, a Xenopus homolog of mouse neuronal leucine-rich repeat protein expressed in the developing Xenopus nervous system. Gene 1998;221:159–66.
26. Fukamachi K, Matsuoka Y, Ohno H, Hamaguchi T, Tsuda H. Neuronal leucine-rich repeat protein-3 amplifies MAPK activation by epidermal growth factor through a carboxyl-terminal region containing endocytosis motifs. J Biol Chem 2002;277:43549–52.
27. Hossain MS, Ozaki T, Wang H, Nakagawa A, Takenobu H, Ohira M, et al. N-MYC promotes cell proliferation through a direct transactivation of neuronal leucine-rich repeat protein-1 (NLRR1) gene in neuroblastoma. Oncogene 2008;27:6075–82.
28. Ishii N, Wanaka A, Tohyama M. Increased expression of NLRR-3 mRNA after cortical brain injury in mouse. Molecular Brain Research 1996;40:148–52.
29. Brodeur GM, Pritchard J, Berthold F, Carlsen NL, Castel V, Castelberry RP, et al. Revisions of the international criteria for neuroblastoma. Diagnosis, staging, and response to treatment. J Clin Oncol 1993;11:1466–77.
30. Matsumura T, Iehara T, Sawada T, Tsuchida Y. Prospective study for establishing the optimal therapy of infantile neuroblastoma in Japan. Med Pediatr Oncol 1998;31:210.
31. Kaneko M, Nishihira H, Mugishima H, Ohnuma N, Nakada K, Kawa K, et al. Stratification of treatment of stage 4 neuroblastoma patients based on N-myc amplification status. Study Group of Japan for Treatment of Advanced Neuroblastoma, Tokyo, Japan. Med Pediatr Oncol 1998;31:1–7.
32. Melino G, Thiele CJ, Knight RA, Piacentini M. Retinoids and the control of growth/death decisions in human neuroblastoma cell lines. J Neurooncol 1997;31:65–83.
33. Thiele CJ, Reynolds CP, Israel MA. Decreased expression of N-myc precedes retinoic acid-induced morphological differentiation of human neuroblastoma. Nature 1985;313:404–6.
34. Niizuma H, Nakamura Y, Ozaki T, Nakanishi H, Ohira M, Isogai E, et al. Bcl-2 is a key regulator for the retinoic acid-induced apoptopic cell death in neuroblastoma. Oncogene 2006;25:5046–55.
35. Bjelfman C, Meyerson G, Cartwright CA, Mellstrom K, Hammerling U, Pahlman S. Early activation of endogenous pp60src kinase activity during neuronal differentiation of cultured human neuroblastoma cells. Mol Cell Biol 1990;10:361–70.

Cancer Science
The official journal of the Japanese Cancer Association

Aberrations of *NEGR1* on 1p31 and *MYEOV* on 11q13 in neuroblastoma

Junko Takita,[1,2,6] Yuyan Chen,[2] Jun Okubo,[2] Masashi Sanada,[3] Masatoki Adachi,[2] Kentaro Ohki,[2] Riki Nishimura,[2] Ryoji Hanada,[4] Takashi Igarashi,[2] Yasuhide Hayashi[5] and Seishi Ogawa[3]

Departments of [1]Cell Therapy and Transplantation Medicine, [2]Pediatrics, and [3]Cancer Genomics Project, Graduate School of Medicine, University of Tokyo, Tokyo; [4]Division of Hematology/Oncology, Saitama Children's Medical Center, Saitama; [5]Gunma Children's Medical Center, Maebashi, Japan

(Received February 9, 2011/Revised May 12, 2011/Accepted May 25, 2011/Accepted manuscript online May 30, 2011/Article first published online July 4, 2011)

MYEOV **and** ***NEGR1*** **are novel candidate gene targets in neuroblastoma that were identified by chromosomal gain in 11q13 and loss in 1p31, respectively, through single nucleotide polymorphism array analysis. In the present study, to assess the involvement of** ***MYEOV*** **and** ***NEGR1*** **in the pathogenesis of neuroblastoma, we analyzed their mutation status and/or expression profiles in a panel of 55 neuroblastoma samples, including 25 cell lines, followed by additional functional studies. No tumor-specific mutations of** ***MYEOV*** **or** ***NEGR1*** **were identified in our case series. Expression of** ***MYEOV*** **was upregulated in 11 of 25 cell lines (44%) and in seven of 20 fresh tumors (35%). The siRNA-mediated knockdown of** ***MYEOV*** **in NB-19 cells, which exhibit high expression of** ***MYEOV,*** **resulted in a significant decrease in cell proliferation (*P* = 0.0027). Conversely, expression studies of** ***NEGR1*** **revealed significantly lower expression of this gene in neuroblastomas at an advanced stage of the disease. Exogenous** ***NEGR1*** **expression in neuroblastoma cells induced significant inhibition of cell growth (*P* = 0.019). The results of these studies provide supporting evidence for** ***MYEOV*** **and** ***NEGR1*** **as gene targets of 11q13 gains and 1p31 deletions in a neuroblastoma subset. In addition, the findings suggest a possible prognostic value for** ***NEGR1*** **in neuroblastoma. (*Cancer Sci* 2011; 102: 1645–1650)**

Neuroblastoma is one of the most common forms of solid tumors in childhood and accounts for approximately 15% of all pediatric cancer deaths.[1] Despite recent advances in chemoradiotherapy, the prognosis for advanced neuroblastoma remains poor, with an approximate 40% 5-year survival, underscoring the importance of developing novel therapeutic modalities on the basis of an understanding of the pathogenesis of neuroblastoma.[1] Conversely, knowledge of the molecular pathogenesis of neuroblastoma is largely limited in terms of targets, except for the role of *MYCN* amplifications in advanced neuroblastoma.[2] Thus, the recent discovery of *ALK* mutations/amplifications in 6–8% of neuroblastomas[3–6] represents a major development in neuroblastoma research because it not only unravels a novel molecular mechanism involved in neuroblastoma development, but could also a basis for the development of molecular-targeted therapies using ALK inhibitors.[3–6] Similar to a number of novel genetic targets discovered recently in other human cancers, *ALK* mutations were identified thorough genome-wide analyses of copy numbers using high-throughput technologies, including high-density single nucleotide polymorphism (SNP) genotyping microarrays.[3–6] A number of recurrent copy number changes other than those of the *ALK* locus have been identified by genome-wide copy number analysis of neuroblastoma, including losses of 1p31, 3q13, 9p24, 15q11, and 16p13, and high-grade amplifications of 1p36, 7q21, 7q31, 11q13, and 15q13,[3] which may provide important clues for the identification of novel target genes. In fact, several candidate target genes of these common deletions and amplifications have been identified, including *MYEOV* as the target of gains/amplifications in 11q13[7] and *NEGR1* as a candidate tumor suppressor in 1p31 deletions.[8] Previously, *MYEOV* was reported as a putative transforming gene within the 11q13 amplicons in multiple myeloma,[9] whereas *NEGR1* was described as a member of the IgLON (limbic system-associated membrane protein [LAMP]/opioid-binding cell adhesion molecule [OBCAM]/neurotrimin subgroup of the immunoglobulin superfamily) family of cell adhesion molecules.[8] However, the involvement of these genes aberrations in the pathogenesis of neuroblastoma remains unknown. Therefore, in the present study we focused on the abnormalities in both genes and assessed their role, both genetically and functionally, in the pathogenesis of neuroblastoma.

Materials and Methods

Specimens. Primary neuroblastoma specimens were obtained at the time of surgery or biopsy from patients who had been diagnosed with neuroblastoma and had been admitted to Tokyo University Hospital, Saitama Children's Medical Center, or various other hospitals between November 1993 and October 2006. Patients were staged according to the International Neuroblastoma Staging System,[10] with five patients classified as Stage 3 and 25 classified as Stage 4. The clinicopathological findings for all patients are listed in Table 1. Twenty-five neuroblastoma cell lines were also used in the present study (Table 2). The SCMC-N2 series was established in our laboratory;[11] the SJNB series and UTP-N-1[12] were generous gifts from Drs A.T. Look (Department of Pediatric Oncology, Dana Farber Cancer Institute, Harvard Medical School, Boston, USA) and A. Inoue (Department of Molecular Biology, Toho University School of Medicine, Tokyo, Japan), respectively; all other cell lines were obtained from the Japanese Cancer Resource Cell Bank (http://cellbank.nibio.go.jp/wwwjcrbj.htm, accessed 7 Sep 2008). All cells were maintained in RPMI 1640 medium (Gibco-BRL, Grand Island, NY, USA) supplemented with 10% fetal bovine serum in a humidified atmosphere containing 5% CO_2 at 37°C.

Semi-quantitative RT-PCR. Total RNA was extracted from the 25 cell lines and 20 frozen stocked tumors using Isogen reagent (Nippon Gene, Osaka, Japan) according to the manufacturer's instructions and was subjected to reverse-transcription reactions to synthesize cDNA using the SuperScript Preamplification System for First Strand cDNA synthesis (Life Technologies, Rockville, MD, USA). Semi-quantitative RT-PCR analysis for *MYEOV*, *CCND1*, and *NEGR1* gene expression was performed as described previously[13] using the primer sets listed in Table S1, available as an accessory publication to this paper. The concentration of the cDNA was normalized against that of *β-actin*, used as an internal control. The signal intensity of *MYEOV* and *CCND1* expression was estimated using NIH

[6]To whom correspondence should be addressed.
E-mail: jtakita-tky@umin.ac.jp

doi: 10.1111/j.1349-7006.2011.01995.x